climate

MDPI

Article

Analysis of Spatial and Temporal Dynamics of Climate Aridization in Rostov Oblast in 1951–2054 Using ERA5 and CMIP6 Data and the De Martonne Index

Denis Krivoguz [1,2,3]

[1] Department of the "Oceanology", Southern Federal University, 340015 Rostov-on-Don, Russia; krivoguz@sfedu.ru
[2] Department of the "Ecological Informatics and Modelling", Donetsk Botanical Garden, 283023 Donetsk, Russia
[3] Department of "Improving Safety and Efficiency of Development of New Regions of the Russian Federation with the Help of Autonomous Transport Mobile Systems", Kherson Technical University, 344049 Genichesk, Russia

Abstract

Rostov Oblast is one of the key grain-producing regions in Russia, accounting for 6% of the total grain production. However, it faces an increasing risk of climate aridization, which requires an accurate scientific assessment to ensure the food security of the country. The present study analyzes the spatial and temporal dynamics of climate aridification in the Rostov region for the period 1951–2054. This analysis is based on ERA5 reanalysis data and CMIP6 forecast models (MPI-ESM1-2-HR, CanESM5, BCC-CSM2-MR). The analysis indicates that the annual mean temperature in the region has increased by 2–3 °C since the 1950s, reaching 12 °C in 2023. At the same time, precipitation shows significant interannual variability with no detectable long-term trend. Spatial analysis reveals a stable meridional temperature gradient and zonality of precipitation distribution. The southeastern parts of the region are characterized by the highest degree of aridification. Projection models indicate further warming (+1.5–3 °C by 2054) and increasing contrasts between western (wetter) and eastern (drier) areas. Projections derived from the CMIP6 models indicate an intensification of aridification, accompanied by a decrease in the De Martonne index of 15–25% by the year 2054. The area of territories with arid climates is expected to increase from 30% to 40%. The most vulnerable regions will be in the southeast part of Rostov Oblast, where the De Martonne index values are predicted to decrease to less than 10. The potential increase in temperature and evapotranspiration, coupled with spatial differentiation, could pose significant risks to the sustainability of the agro-industrial complex, particularly in the southeastern part of the region.

Keywords: aridization; Rostov Oblast; climate change; De Martonne index; desertification; ERA5; CMIP6

check for updates

Received: 10 June 2025
Revised: 3 July 2025
Accepted: 17 July 2025
Published: 17 July 2025

Citation: Krivoguz, D. Analysis of Spatial and Temporal Dynamics of Climate Aridization in Rostov Oblast in 1951–2054 Using ERA5 and CMIP6 Data and the De Martonne Index. *Climate* **2025**, *13*, 151. https://doi.org/10.3390/cli13070151

Copyright: © 2025 by the author. Licensee MDPI, Basel, Switzerland. This article is an open access article distributed under the terms and conditions of the Creative Commons Attribution (CC BY) license (https://creativecommons.org/licenses/by/4.0/).

1. Introduction

Aridization is defined as a global process of decreasing moisture availability in territories. This phenomenon has become a major challenge in the 21st century. According to recent studies, arid lands cover 41% of the Earth's land surface [1,2], and their area may increase by 12–23% by 2100 [1,3]. Anthropogenic climate change has already degraded 5.43 million km^2 of drylands [4], affecting the livelihoods of about 213 million people living

mainly in developing countries [4,5]. These trends are further intensified by the increasing frequency of extreme droughts: 4500 meteorological droughts were recorded between 1951 and 2016, with 52 of these classified as mega-droughts [6]. In 2023, 48% of the global landmass will experience at least one month of extreme drought [7], while forecast studies indicate an intensification of this trend in temperate latitudes [3,8].

Aridization studies of the modern era are dependent on syntheses of climate reanalysis data and projection models to reconstruct past conditions and project future scenarios. The ERA5 reanalysis has become a key tool due to its high spatial and temporal resolution and ability to reproduce temperature trends with less than 5% error, even in complex geographic environments [9,10]. Its modification, ERA5-Land, with 9 km resolution, demonstrates high accuracy in air temperature estimates (R^2 = 0.92 for mountainous areas), although precipitation is characterized by systematic overestimation by 15–40% in regions with pronounced relief [10]. The CMIP6 represents the latest phase of the Coupled Model Intercomparison Project, which aims to enhance the capabilities of climate process modeling. CMIP6 data have been utilized in various studies examining regional aridification and drought, demonstrating their efficacy in analyzing changes in aridity indices, particularly in arid regions [11,12]. For example, a study in Ethiopia utilized an ensemble of three CMIP6 global climatic models, demonstrating a high level of effectiveness in predicting aridity and evapotranspiration change up to 2070 [11]. Additionally, a series of studies have demonstrated the effectiveness of CMIP6 data in analyzing extreme climatic phenomena. Studies have demonstrated the reproducibility of atmospheric rivers [13], drought risks [14,15], and atmospheric circulation patterns [16,17]. For instance, research conducted in China indicated that the CMIP6 model demonstrated adequate reproducibility in simulating the spatial distribution of precipitation and temperature [14].

The quantitative evaluation of aridization is based on various indices, each of which has its own advantages and disadvantages. Simple climatic indices, such as Lang's or the De Martonne aridity indices, are characterized by ease of calculation and minimal requirements for data [18,19]. Evapotranspiration-based indices, such as the UNEP and Emberger aridity indices, offer a physically justified evaluation; however, they require additional meteorological parameters for complete analysis [19,20]. Standardized indices (SPI and SPEI) facilitate multi-scale analysis; yet, the SPI does not consider the effects of temperature, while the SPEI is characterized by its calculation complexity [21,22]. The De Martonne index was selected for the present study due to several factors, including its optimal balance between simplicity and physical validity, its proven effectiveness in continental climate conditions [19], its compatibility with ERA5 and CMIP6 data on long time series, and its relevance for agricultural applications in the steppe zone. Despite the limitations of the index (which exclude the consideration of seasonality in precipitation and evapotranspiration processes), its use is valid for regional analysis of aridization in continental climate conditions [23,24].

The Rostov region plays a very significant role in the agro-industrial sector of the economy of the Russian Federation and is characterized by high temperatures and low precipitation. According to [25] research results, the increase in average temperature in the Rostov region reached 1.2 °C in the period from 1966 to 2020, while the precipitation level remained the same. On the other hand, projections indicate the possibility of an increase in the number of potential droughts in the region, reduced crop yields, and a shift in climate regime between 2030 and 2050 [26]. Analysis of historical data by Gudko [27] and Nazarenko [28] indicates a tendency for temperatures to rise significantly, especially during the warm summer months, leading to the formation of significant areas of drought in areas such as Giant, Rostov-on-Don, Taganrog, and Tsimlyansk. The presence of arid conditions within the Rostov region is also indicated by the Seljaninov hydrothermal coeffi-

cient, which measures the relationship between temperature and precipitation. According to Gudko's calculations [27], based on the values of this indicator, aridity is characteristic of most of the territory of the region, where its value varies from 0.64 to 0.82, with the driest conditions observed in the eastern and northeastern parts of the region. Such peculiarities of the climate determine the presence of several problems, the most prominent of which are desertification and changes in the state of soil resources. Thus, the problem of desertification is particularly acute in such districts as Zavetinsky, Remontnensky, Dubrovsky, Zimovnikovsky, and Orlovsky. The total area affected by desertification is about six million hectares, which has an impact on soil properties and agricultural productivity [29]. Furthermore, an increase in evaporation rates has been observed to intensify the processes of salinization and alkalinization in chernozem and chestnut soils, particularly within irrigated regions [30]. Although the climate of Rostov Oblast is relatively stable, the region is still facing challenges primarily related to water availability and desertification, which have a significant impact on agriculture and environmental management in this region.

Despite the recognized importance of aridization processes for the agro-industrial complex of the southern regions of Russia, there is no comprehensive assessment of the spatio-temporal dynamics of climatic aridization in the Rostov region based on modern high-resolution data and long-term climatic projections. The existing studies are limited to fragmentary analysis of individual climatic parameters without an integral assessment through specialized aridity indices.

Research gaps include the absence of long-term analysis based on high-resolution data, the lack of up-to-date climate projections for the region, and the absence of spatially differentiated adaptation strategies for the agricultural sector.

The scientific novelty lies in the first comprehensive 73-year aridification analysis for the region using the De Martonne index and the integration of three CMIP6 models for 30-year projections, which provides a scientific basis for developing adaptation strategies.

The working hypothesis is that the spatio-temporal dynamics of aridization in the Rostov region are characterized by a stable southeastern gradient, with the maximum intensity of processes occurring in the Manych lowland. This requires geographically differentiated adaptation measures in the agro-industrial complex.

The goal of this study was to comprehensively assess the spatial and temporal dynamics of climate aridization in the Rostov region. To achieve this, the study analyzed historical data from 1951 to 2024 and used predictive climate models from 2025 to 2054. The analysis produced scientifically based recommendations for the adaptation of the region's agro-industrial complex.

To achieve this goal, the following tasks were completed:

The present study aims to utilize ERA5 reanalysis data to assess the historical trends of temperature, precipitation, and the De Martonne aridity index in the Rostov region for the period 1951–2024.

The identification of spatial patterns of aridization shall be achieved through the analysis of meridional gradients of thermal regime, precipitation distribution, and De Martonne index values.

A comprehensive analysis of CMIP6 projection data, including MPI-ESM1-2-HR, CanESM5, and BCC-CSM2-MR, is essential for evaluating the potential scenarios of aridization in the Rostov region.

2. Materials and Methods

2.1. Characterization of the Study Area

Rostov Oblast is located in the southern part of Russia, in the southern part of the East European Plain, and is part of the Southern Federal District. Geographically, the region

is situated between 46° and 50° north latitude and between 38° and 43° east longitude, a position that serves as a significant transportation and economic hub, connecting central Russia with the Caucasus and the Black Sea region (Figure 1). The topography of the Rostov region is characterized by a pronounced asymmetry, with the northern and western parts of the region, including the Kalachskaya Upland and the Donetsky Ridge, elevated to 200–250 m above sea level, while the southern and southeastern areas fall to 0–50 m. The geographical division between these zones is defined by the Lower Don Valley, which intersects the region from northeast to southwest.

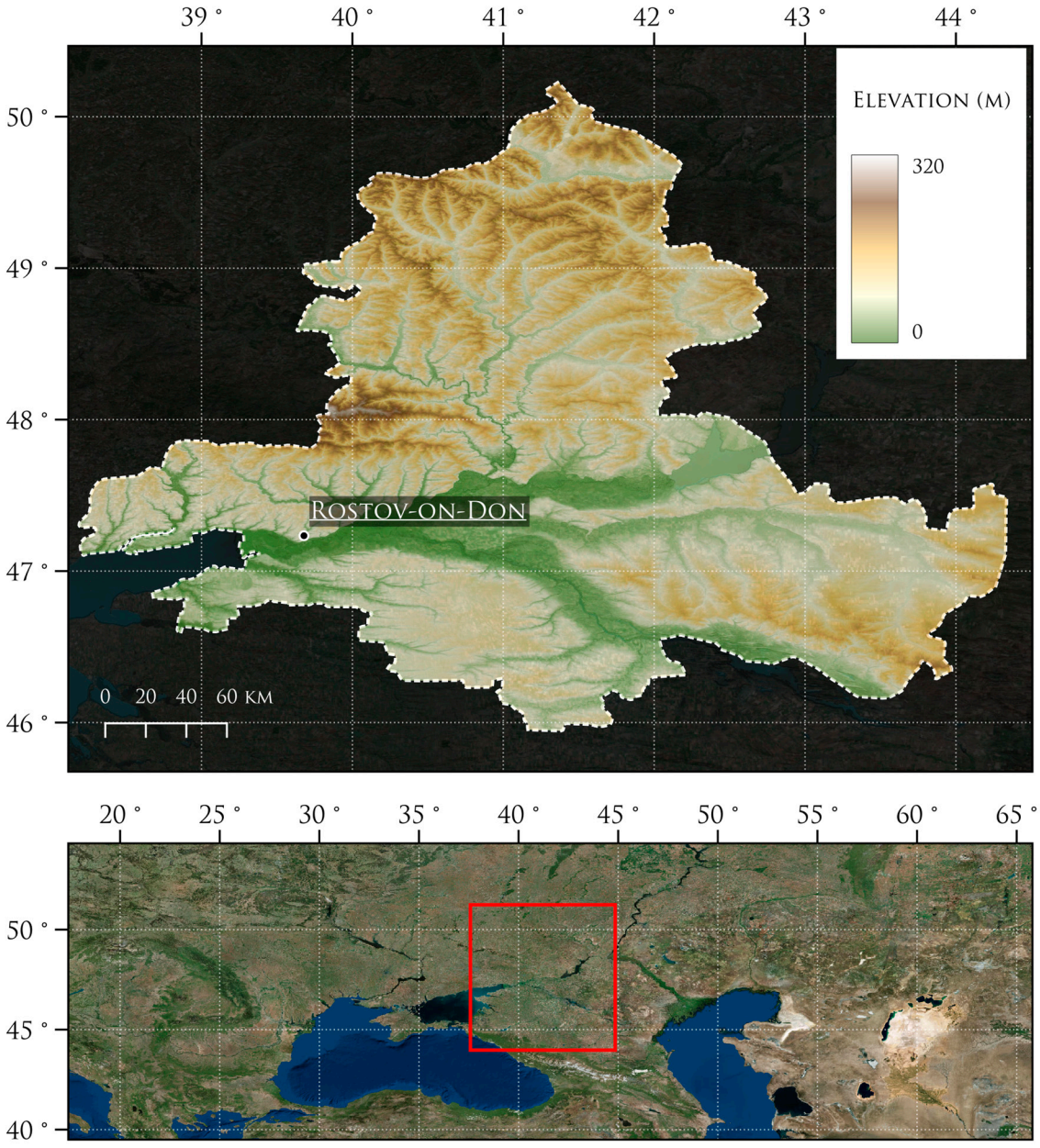


Figure 1. The geographical location of the research area, with the corresponding elevation data. The red square represents the location of the research area.

The Rostov region is characterized by a temperate continental climate, which is characterized by aridity and significant variability of temperature and precipitation regimes [31]. According to the Köppen classification, the climate of the Rostov region is classified as Dfa, which is characteristic of an area with a humid continental climate, featuring warm summers and cold winters. According to long-term observations, the average annual air

temperature in this region is approximately 11.2 °C, with July being the warmest month and January the coldest [25]. Precipitation in the Rostov region is characterized by its year-round uniformity.

Agriculture is one of the primary drivers of economic development in the region [32,33]. The Chernozems, covering 65% of the territory [34], are responsible for the production of 11% of the total grain yield in Russia [35,36]. The annual harvest of wheat exceeds 10.55 million tons [36], while barley yields reach approximately 0.9 million tons, according to Rosstat. Livestock breeding is focused on meat and dairy production: the number of cattle is 420 thousand, pigs—680 thousand, sheep—1.2 million, according to Rosstat data. The fishing industry, using the resources of the Sea of Azov and Tsimlyansk reservoir, provides a large amount of the freshwater fish catch in Russia, including pikeperch and bream [37]. The region's foreign economic activity is focused on the export of agricultural products, metals, and engineering machinery [38]. The oblast's share in Russia's grain exports is 12% [35].

2.2. Scheme of the Study

The De Martonne aridity index was employed to quantitatively assess the degree of moisture content in the territory. This index was calculated using the following formula [39]:

$$AI_{DM} = \frac{P}{(T + 10)} \quad (1)$$

where AI_{DM}—De Martonne aridity index, P—annual precipitation in mm, and T—average annual air temperature in °C. A primary motivation for selecting this aridity index is its capacity to concurrently consider temperature and precipitation variables. This capability is supported by extensive research demonstrating its significance for the examination of aridization [40,41]. Furthermore, it is quite useful for the purpose of comparing the relative moisture conditions of areas that exhibit disparate thermal regimes [40,42].

Despite its numerous advantages, the index does have several disadvantages. Firstly, it is important to note that this index does not consider the seasonal distribution of precipitation, which may result in an overestimation of moisture content in regions experiencing significant summer drought [41,42]. A careful approach is also necessary in harsh climates with extremely low average annual temperatures $T < -10$ °C.

The interpretation of the De Martonne aridity index is presented in Table 1.

Table 1. Classification of the De Martonne index depending on its values.

Climate Type	De Martonne Aridity Index Values
Arid	$AI_{DM} < 10$
Semi-Arid	$10 \leq AI_{DM} < 20$
Mediterranean	$20 \leq AI_{DM} < 24$
Semi-Humid	$24 \leq AI_{DM} < 28$
Humid	$28 \leq AI_{DM} < 35$
Very Humid	$35 \leq AI_{DM} < 55$
Extremely Humid	$AI_{DM} > 55$

The De Martonne index was calculated using the data presented in Table 2, which was obtained from the Google Earth Engine (GEE) cloud platform.

Table 2. Characterization of the data used in this study.

Name	Dataset Name	Variable Name	Model
ERA5-Land Monthly Aggregated—ECMWF Climate Reanalysis	ECMWF/ERA5_LAND/ MONTHLY_AGGR	temperature_2m total_precipitation_sum	- -
NEX-GDDP-CMIP6: NASA Earth Exchange Global Daily Bias-Corrected and Downscaled Data	NASA/GDDP-CMIP6	tas pr	MPI-ESM1-2-HR, CanESM5, BCC-CSM2-MR

Temperature and precipitation data for the period from 1951 to 2024 were obtained from the ERA5 reanalysis dataset with a spatial resolution of 0.25° × 0.25°, and the forecast values for 2025–2054 were calculated using the MPI-ESM1-2-HR, CanESM5, and BCC-CSM2-MR models from the CMIP6 dataset.

The selection of models was determined by several criteria, including the availability of the NEX-GDDP-CMIP6 archive for all utilized variables, the range of climatic sensitivity levels (from moderate in BCC-CSM2-MR to high in CanESM5), and the proven effectiveness of these models in reproducing climate parameters in the European part of Russia [43–45]. The models also show the lowest errors in reproducing temperature trends and precipitation regimes in the European part of Russia (MPI-ESM1-2-HR has an average error of ±0.5 °C) [46,47]. The BCC-CSM2-MR model is often considered to be among the top five models for continental climate analysis [48–50]. It has been demonstrated to be highly effective in capturing diurnal temperature variations in regions where grain production is a significant economic driver, making it a valuable tool for agricultural applications. MPI-ESM1-2-HR is characterized by its high spatial resolution and effective performance in temperature projections, yet it demonstrates certain inaccuracies in precipitation predictions, attributable to systematic biases [51,52].The CanESM5 model is associated with "hot models", which are characterized by a climatic sensitivity of 5.65 K, a value that is higher than that of all CMIP6 models [53]. Consequently, it can be considered a scenario of the highest border of warming.

CMIP6 data were obtained from the NEX-GDDP-CMIP6 archive, where the Bias Correction Spatial Disaggregation (BCSD) method was applied. The processing procedure included two primary steps [54,55]. In the first step, quantile mapping was applied for each variable by comparing the cumulative distribution functions (CDF) of the model data and the Global Meteorological Forcing Dataset (GMFD) observations for the period 1960–2014. To ensure the integrity of the data, a nine-year moving average was employed for each month to calculate long-term trends. In the second step, interpolation was performed from the native resolution of the models to a 0.25° × 0.25° grid. This process preserved the spatial detail of the observational data by applying scaling factors to the high-resolution GMFD climatology.

Both datasets were acquired through the GEE cloud platform using the Python libraries geemap (v. 0.30.0), xarray (v. 2024.7.0), and xee (v. 0.0.20). Initially, the data underwent averaging of monthly values to annual values—for temperature, these were the mean values, and for precipitation, the sum. To analyze long-term trends, decadal averages were calculated for all parameters.

3. Results

3.1. Historical Climate and Aridity Analysis (1951–2024)

The temperature regime in Rostov Oblast from 1951 to 2024 demonstrated significant variability, with a pronounced positive trend, particularly evident in the last two decades (Figure 2). At the beginning of the study period in the 1950s, the mean annual temperature fluctuated primarily within the range of 8–10 °C, with an absolute minimum of 7 °C

recorded in 1956. During the three decades that followed, up to 1990, the temperature regime was characterized by quasi-cyclical fluctuations without a particularly pronounced trend, with periodic decreases to 6.7 °C in 1987 and increases to 10.7 °C in 1966.

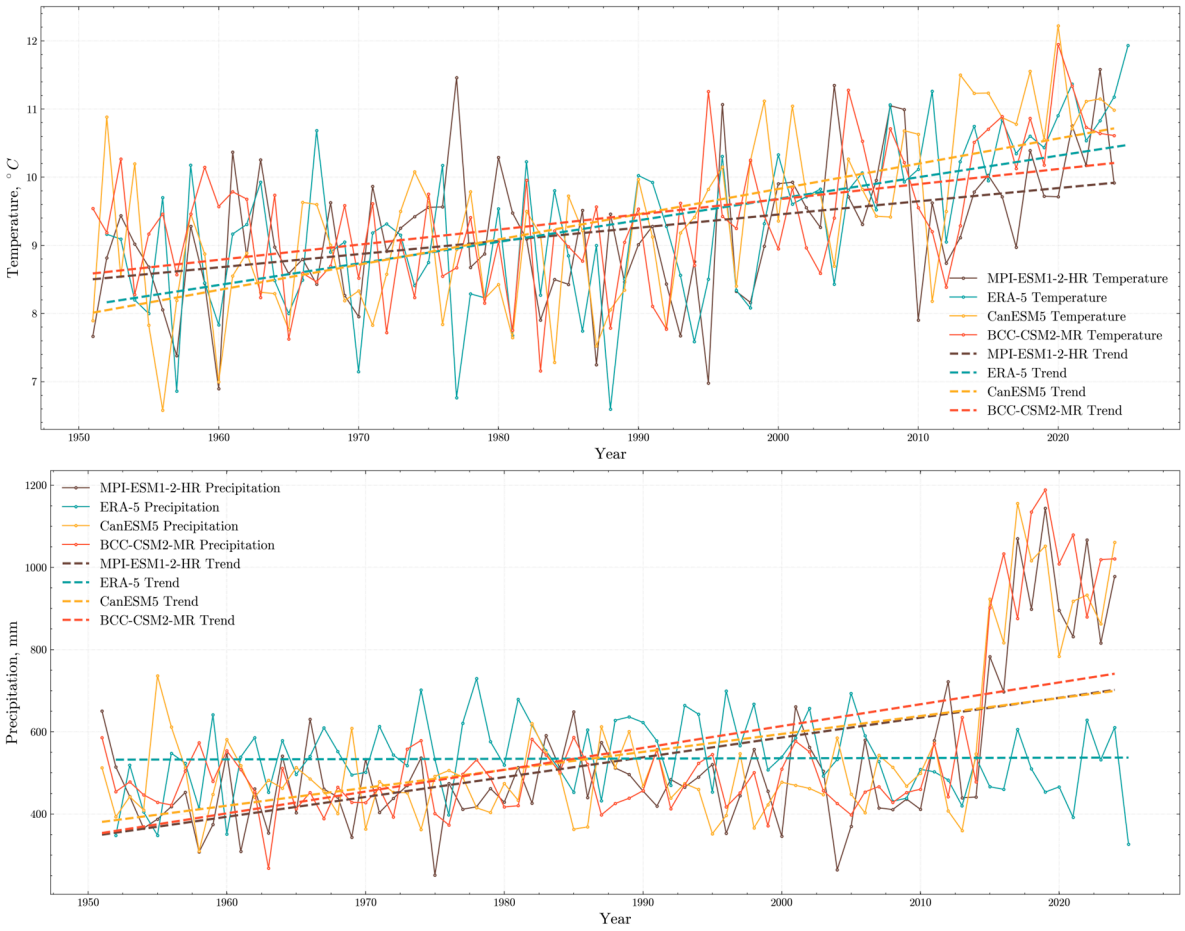


Figure 2. Distribution of mean annual temperature and precipitation averaged over the Rostov region from 1951 to 2024 according to ERA5 and CMIP6 data.

The warming process intensified significantly in the early 2000s. Consequently, the final stage of the period under investigation is marked by a pronounced increase in the mean annual air temperature, with values regularly exceeding 10 °C, reaching 11 °C and higher in certain years. The maximum recorded for the entire observed series was in 2023, at approximately 12 °C, which is several degrees above the minimum values recorded in the middle of the twentieth century.

In contrast to the temperature series, precipitation does not demonstrate a clear unidirectional trend, which is reflected in high interannual variability. The minimum values of precipitation were recorded in the early 1950s and amounted to 320–350 mm, as well as at the end of the period under study. The maximum values were observed in the late 1970s, and exceeded 700 mm. A particularly pronounced increase in precipitation is observed in the Rostov region from 1970 to 1985, with several distinct peaks reaching over 700 mm per year. In the late twentieth and early twenty-first century, the amplitude of fluctuations has been observed to decrease, with periodically repeatable peaks in certain years.

The graphical representations of both variables demonstrate a decline in precipitation accompanied by an increase in temperature in the early twenty-first century. This indicates an increase in continentality and a shift towards a drier climate in the Rostov region.

The analysis of the spatial distribution of temperatures in the Rostov region demonstrates a stable zonal structure of the thermal field (Figure 3). A meridional temperature

gradient is evident in all periods under analysis, with increasing values from north to south. The lowest temperatures in the northern parts of the region, which border the Voronezh and Volgograd regions, are typically in the range of 8–9 °C. In contrast, the southern territories that border the Azov Sea exhibit higher temperatures, ranging from 10–11 °C. The primary cause of this differentiation is predominantly attributed to the latitudinal location of the region, as well as the influence of continental-marine climatic contrasts. The mitigating effect of the Azov Sea is manifested in the formation of a relatively warm zone in the southern part of Rostov Oblast, which is especially evident in Taganrog Bay. In contrast, the northeastern regions demonstrate a more pronounced continental influence, characterized by lower temperature values.

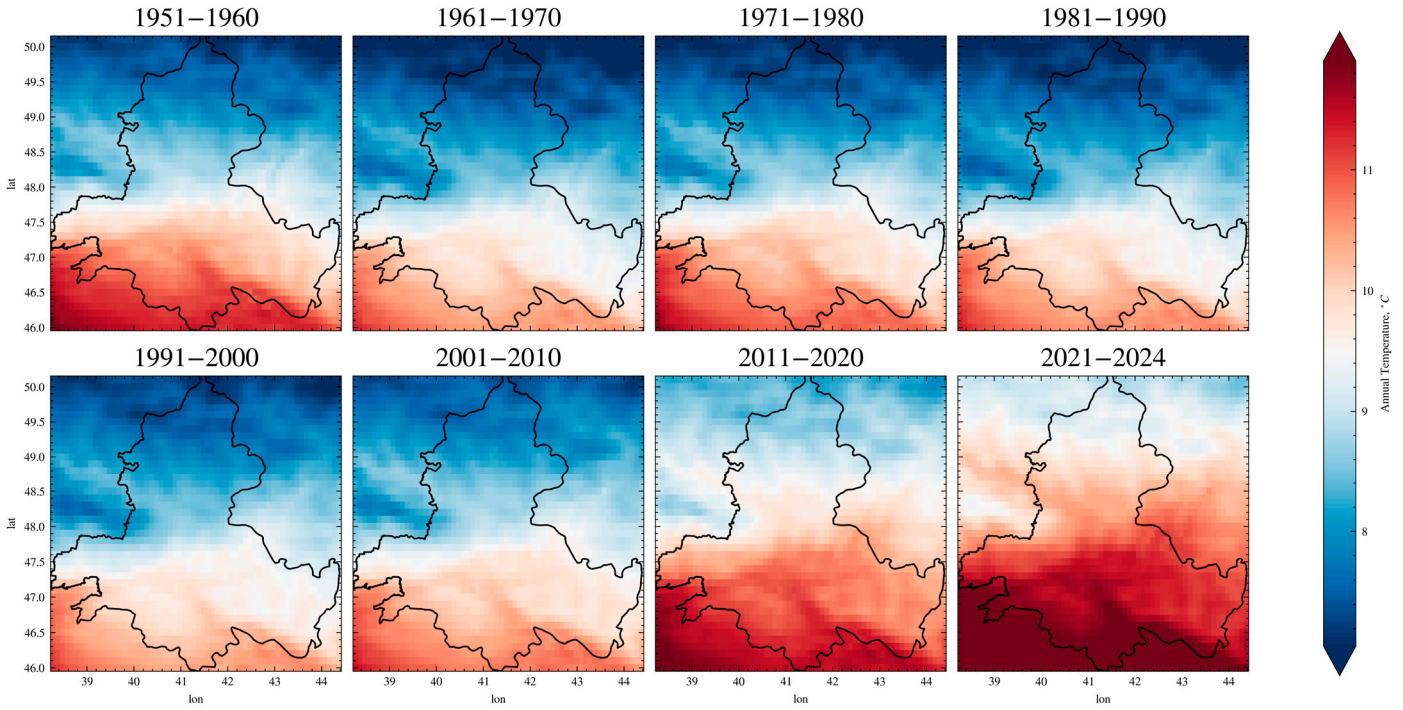


Figure 3. Spatial distribution of air temperature according to ERA5 data on the territory of Rostov Oblast for ten-year periods from 1951 to 2024.

Analysis of the spatial distribution of precipitation in Rostov Oblast reveals a relatively uneven structure (Figure 4). Large values prevail mainly in the southwest in the areas adjacent to the Sea of Azov and the Gulf of Taganrog, reaching average annual values of 650 mm in some years.

The northern parts of the region are characterized by lower values of approximately 350–500 mm, with some years reaching 500–550 mm. The southeastern region is the most arid, with average annual precipitation levels rarely exceeding 400–450 mm. The distribution of precipitation is influenced by the same factors as temperature, including proximity to the Azov Sea in the south and continental climate in the north.

The distribution of the De Martonne index across the Rostov region from 1951 to 2024 was found to be non-uniform (Figure 5). Therefore, from 1951 to 1960, most of the Rostov region demonstrated minimal values for the index, indicating arid climatic conditions. The minimum values of aridity were observed in the southeastern region.

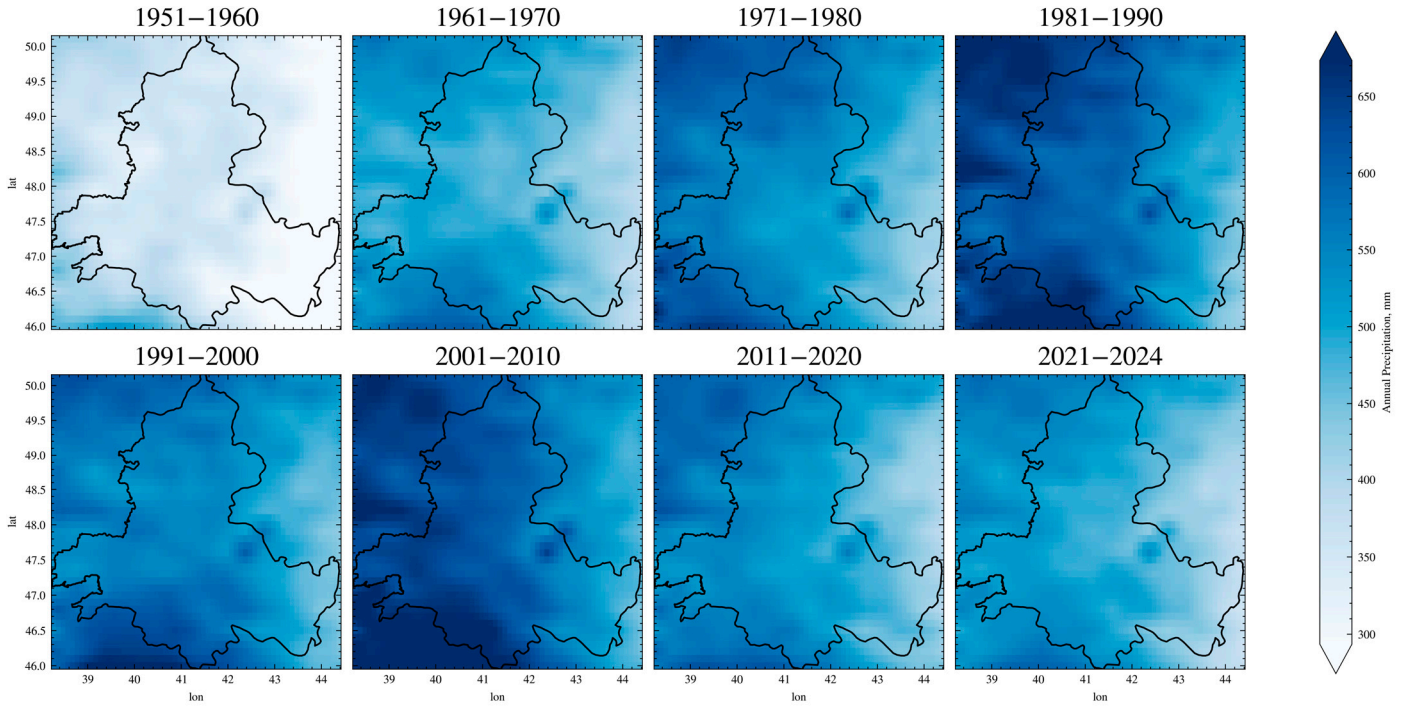


Figure 4. Spatial distribution of annual precipitation according to ERA5 data on the territory of Rostov Oblast for ten-year periods from 1951 to 2024.

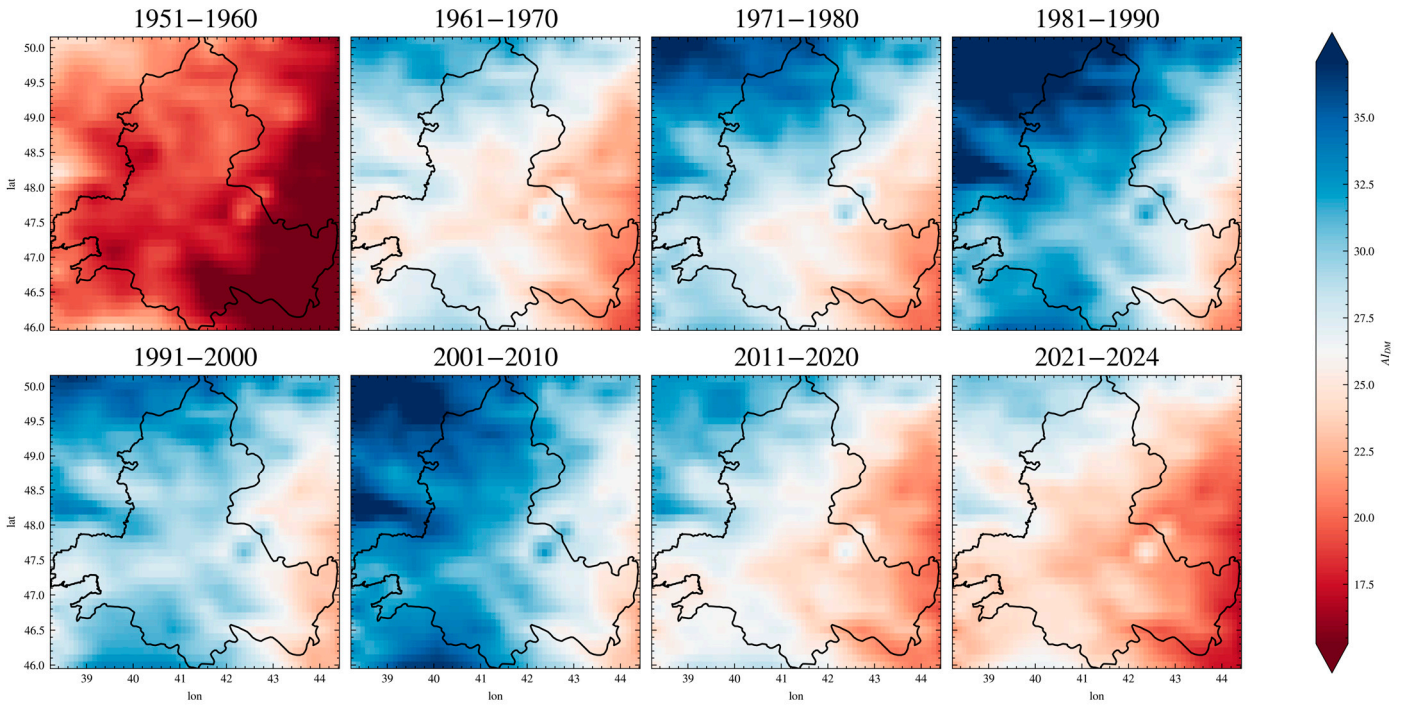


Figure 5. Spatial distribution of the De Martonne index according to ERA5 data on the territory of Rostov Oblast for ten-year periods from 1951 to 2024.

From the 1960s to the 1980s, there was a consistent increase in the De Martonne index, with a gradual rise from west to east. By the late 1980s, the greater part of the region had already become characterized by relatively humid conditions, indicating a decrease in aridity trends in the area. However, it is important to note that climatic conditions in the southeast remained predominantly arid. During the 1990s and 2000s, trends toward a wetter climate persisted throughout the region, reaching a maximum over the entire study

period. In contrast, the De Martonne index has demonstrated a substantial decrease across the region, particularly in the southeastern areas, suggesting a resumption of the gradual aridification of the region.

It is important to note that throughout the entire period of observations, a clear trend is identified: the less arid conditions are observed in the northwestern and western regions, while the southern regions typically experience higher levels of aridity. Furthermore, an analysis of the temporal dynamics reveals a shift in the boundary between wetter and drier zones to the northwest, suggesting an expansion of arid conditions across a more extensive region.

3.2. Future Climate and Aridity Scenarios (2025–2054)

The graphs presented in Figures 6 and 7 offer a comparison of historical data from the ERA5 reanalysis with projections from three global climate models for the period 2025–2054 for the Rostov region. According to calculations derived from the MPI-ESM1-2-HR model, the mean annual temperature in Rostov Oblast is projected to increase from its current value of approximately 11 °C to a range of 11.5–12.0 °C by the year 2054. The model demonstrates a relatively moderate rate of warming, accompanied by minimal interannual variability. A distinguishing attribute of this scenario is the gradual and consistent rise in temperature, which is indicative of a systematic adjustment of the regional climate system to evolving environmental factors.

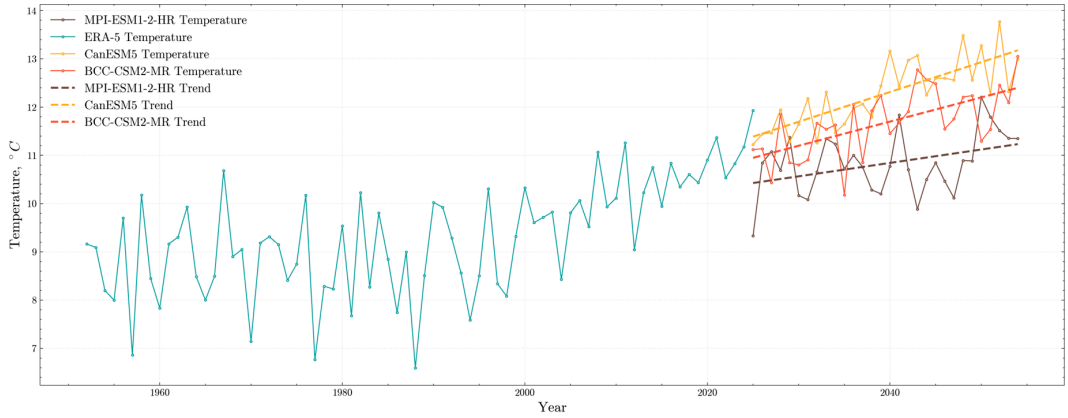


Figure 6. Comparison of ERA5 reanalysis data with temperature projections of three global climate models, MPI-ESM1-2-HR, CanESM5, and BCC-CSM2-MR.

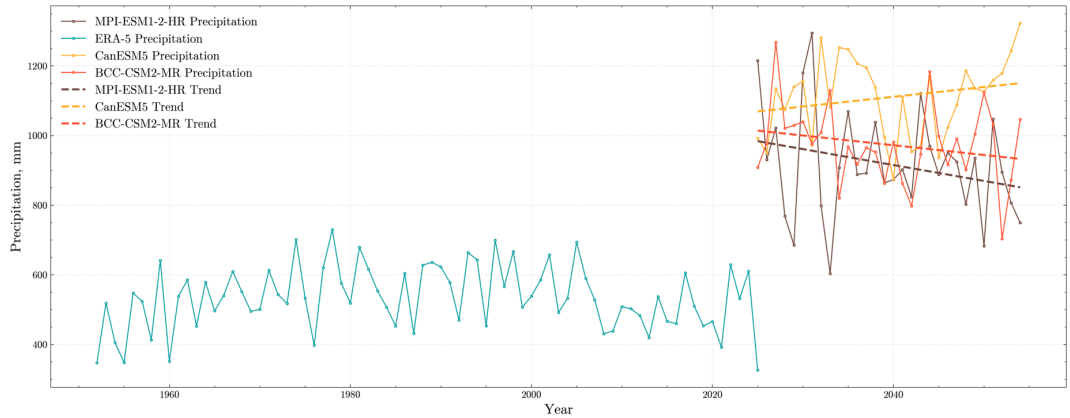


Figure 7. Comparison of ERA5 reanalysis data with forecast calculations of precipitation from three global climate models, MPI-ESM1-2-HR, CanESM5, and BCC-CSM2-MR.

The CanESM5 model anticipates the most intense warming among the considered scenarios. The mean annual temperature is projected to increase from 12 °C in 2025 to 13.5–14.0 °C by 2054, representing an increase of 1.5–2.0 °C over the 30-year period. The model is distinguished by significant interannual variability, with temperature fluctuations ranging from ±0.5 to 1.0 °C relative to the trend. This scenario is predicated on a substantial transformation of climatic conditions in the region.

The BCC-CSM2-MR model occupies an intermediate position between the two previous scenarios. The projected temperature increases range from 11.5 °C at the beginning of the period to 12.5–13.0 °C by 2054. The model demonstrates moderate interannual variability and a relatively stable warming trend, indicating that this scenario is the most probable to maintain current climate trends.

According to calculations performed using the MPI-ESM1-2-HR model, there will be significant changes to the precipitation regime in Rostov Oblast. The model predicts an increase in the interannual variability of annual precipitation amounts compared to the historical period. The mean annual precipitation in this region is approximately 600–900 mm, which is significantly higher than the most observed values during the XX–early XXI century (400–600 mm). In certain years, maximum precipitation levels have been observed to reach up to 1000–1200 mm, while minimum values have not decreased below 600 mm.

The CanESM5 model also demonstrates an increasing trend in annual precipitation amounts. In the forecast period, the values in most years are in the range of 600–1000 mm, and by the end of the period (2045–2054), there is a further increase, up to 1100–1200 mm in some years. Interannual variability is high, indicating a possible increase in both very wet and relatively dry years. A general analysis indicates that the CanESM5 scenario projects the most significant increase in precipitation among the models under consideration.

According to the BCC-CSM2-MR model, the annual precipitation is projected to increase between 2025 and 2050 compared to the historical period. However, the range of variability is expected to be more extensive, primarily between 700 and 1000 mm, with some extremes reaching up to 1300 mm. Interannual variability is observed and found to be more pronounced than in the CanESM5 scenario. The model confirms the general trend of increasing precipitation, but to a more significant extent than the other scenarios.

The spatial distribution of temperature and precipitation in the Rostov region, as predicted by global models, is illustrated in Figures 8 and 9. The results of the MPI-ESM1-2-HR model demonstrate that in the initial period (2025–2034), the conventional meridional temperature gradient, characterized by cooler conditions in the northern regions (8–9 °C) and higher temperatures in the southern part (10–11 °C), is sustained within the region. In the subsequent period (2035–2044), a pronounced warming trend is observed, particularly evident in the southern and central regions. For a large area, an average annual temperature of 11–12 °C becomes the norm, which is 2–3 °C higher than in the previous period. By the late 2040s and early 2050s, the projected temperature increase will have a significant impact on nearly the entire region. Notably, even the northern regions, traditionally known for their low temperatures, are experiencing values of 10–11 °C, while the southern territories are reaching 12–13 °C.

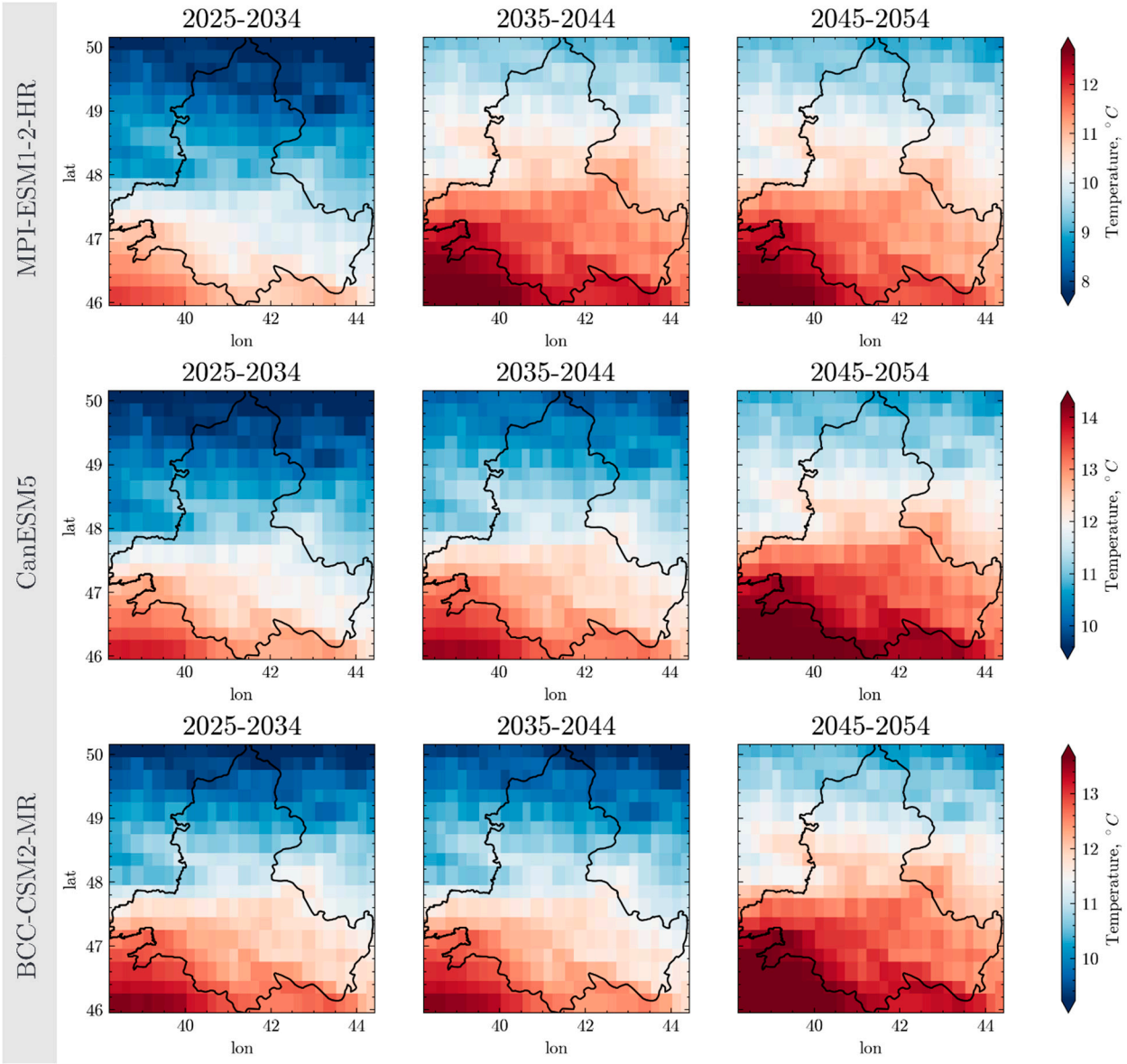


Figure 8. Spatial distribution of air temperature according to the global climate models MPI-ESM1-2-HR, CanESM5, and BCC-CSM2-MR in Rostov Oblast for ten-year periods from 2025 to 2054.

The CanESM5 model projects a more moderate rate of warming over the next decade. This period is distinguished by relatively stable temperature conditions, accompanied by the retention of the natural latitudinal temperature gradient, where temperatures range from 9 to 11 degrees Celsius. From 2035 to 2044, there will be a gradual increase in temperature, with the northern parts of the region maintaining relatively cool conditions. The most pronounced warming has been observed in the central and southern regions of the region. During the period 2045–2054, a marked warming is observed throughout the region, particularly in the southern part. The range of temperature distribution during this period is observed to be at its peak between 11 and 14 °C.

The BCC-CSM2-MR model demonstrates notable similarities to CanESM5 in many aspects, with the exception of the final period. The temperature profile across the region is characterized by a gradual increase, with a meridional gradient extending from north to south. The final period is distinguished by a substantial increase in temperature relative to CanESM5, yet in this instance, the range of variability is narrower, spanning from 10 to 13 °C.

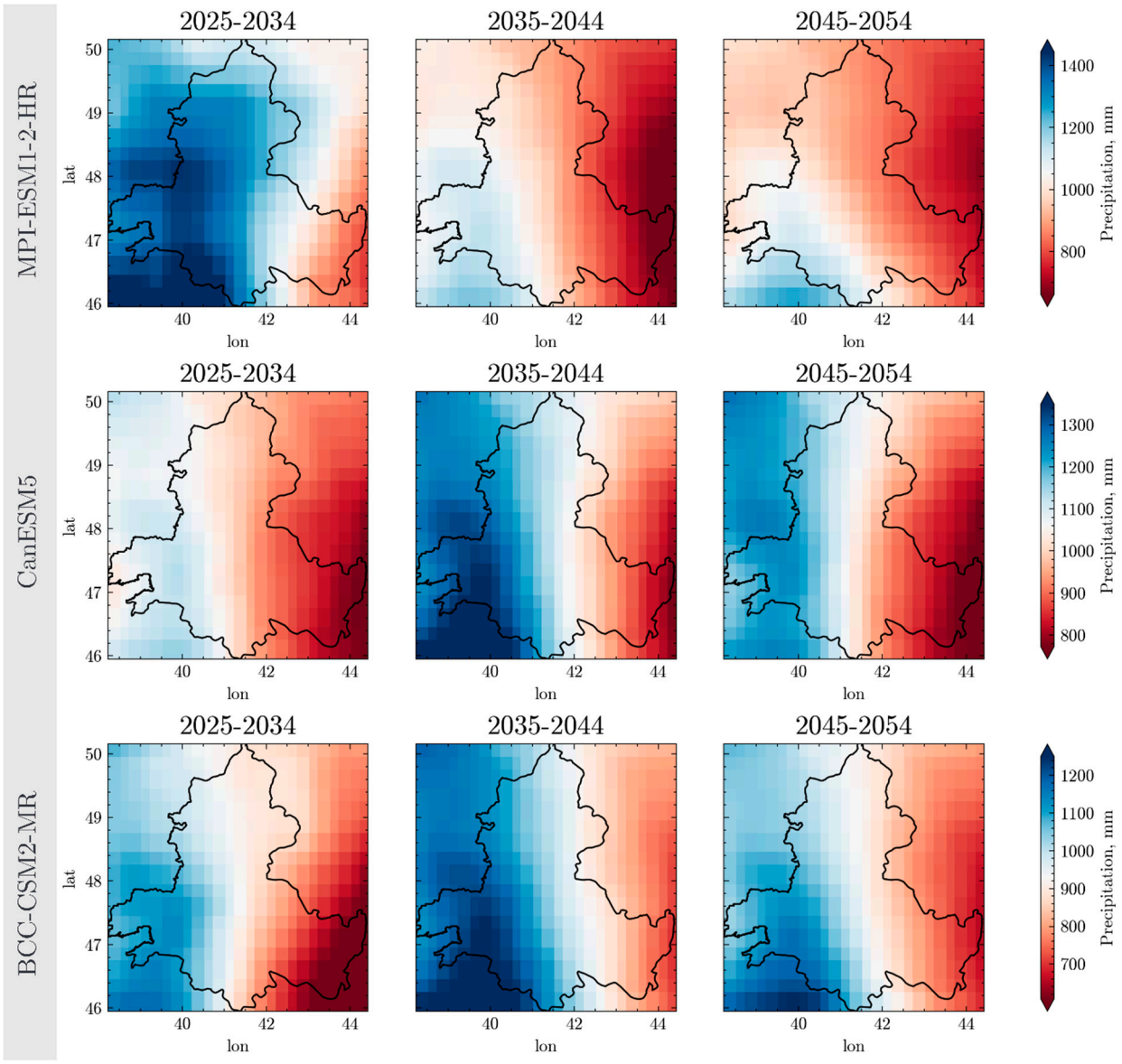


Figure 9. Spatial distribution of precipitation according to the global climate models MPI-ESM1-2-HR, CanESM5, and BCC-CSM2-MR in Rostov Oblast by decade from 2025 to 2054.

The distribution of precipitation varies among the models as well. According to calculations derived from the MPI-ESM1-2-HR model, a pronounced zonal precipitation gradient is expected to form in the Rostov region during the initial period (2025–2034). The precipitation levels in the western and northwestern regions are notably higher, with annual amounts ranging from 1200 to 1400 mm. In contrast, the eastern and southeastern territories exhibit significantly lower precipitation levels, with annual totals ranging from 800 to 1000 mm. From 2035 to 2044, a fundamental shift will occur in the spatial distribution of precipitation. A substantial decline in annual precipitation levels (800–1000 mm/year) has been documented across the region. A pronounced decrease in precipitation has been observed, particularly in the western regions that were previously characterized by high precipitation levels. By the mid-1960s of the 21st century, the trend toward aridization intensifies. The eastern parts of the region demonstrate critically low precipitation values (700–800 mm/year), while the western part exhibits slightly more favorable moisture conditions (900–1000 mm/year).

The CanESM5 model demonstrates substantially different spatial dynamics of precipitation. From 2025 to 2034, a contrast between drier eastern regions and relatively wetter western regions is also evident. However, this contrast is less pronounced compared to that observed in the MPI-ESM1-2-HR model. The period between 2035 and 2044 is characterized by an increase in spatial differentiation. The western and northwestern parts of the region are characterized by increased precipitation levels, with annual precipitation amounts exceeding 1200 mm. In contrast, the eastern half of the territory exhibits moderately arid conditions. In the final period (2045–2054), the spatial structure stabilizes with the preservation of a pronounced west–east gradient. The western regions are distinguished by a high degree of moisture, which can be indicative of changes in cyclone trajectories and alterations in the regional atmospheric circulation.

The BCC-CSM2-MR model demonstrates the most conservative dynamics of the spatial distribution of precipitation. In the period 2025–2034, most of the region is characterized by a relatively uniform distribution of precipitation, ranging from 900 to 1100 mm/year, with minimal fluctuations. Following this period, a gradual increase in total precipitation is evident, particularly in the western part of the region. By the end of the period, a moderate gradient is expected to have formed, with wetter conditions predominating in the west and northwest of the region.

Therefore, the findings of the analyzed models indicate warming, yet the intensity of this warming varies among the models. The CanESM5 model predicts the most significant increase in temperature, while the other two models project more moderate increases. In the context of precipitation, a similar situation is observed. CanESM5 predicts a differentiation between the west and east in terms of precipitation. MPI-ESM1-2-HR predicts a progressive decrease in humidity after its rapid increase in the first 10 years. BCC-CSM2-MR shows more restrained scenarios of precipitation increase compared to the first two.

The identified spatial patterns suggest a potential transformation of regional climate systems. The strengthening of temperature gradients and changes in the spatial pattern of precipitation may lead to the formation of new agroclimatic zones. This, in turn, may require a revision of land use strategies in different parts of Rostov Oblast. The western regions of the region may encounter issues related to overwatering or, conversely, moisture deficit, while the eastern areas are susceptible to increasing aridity under all scenarios.

The De Martonne aridity index demonstrates significant variation across models (Figure 10). Consequently, the MPI-ESM1-2-HR model demonstrates the most significant variability among aridity classes, both geographically and temporally. Projections indicate that between 2025 and 2034, the region's territory will undergo a substantial increase in moisture content, with the western part predominantly comprising areas characterized by a very humid climate. The region's territory is characterized by a notable presence of moisture, with no arid regions observed during this period. The transition to the next time stage is accompanied by a significant change in climatic characteristics. Although arid conditions are not yet present, the parameters have already fallen to the boundary of aridity limits, initially in the southeastern region of the oblast, where the index value is 30–40 units. In the last period, climatic conditions changed slightly, making the climate more humid than in the previous period, and the index value is between 45–50 units.

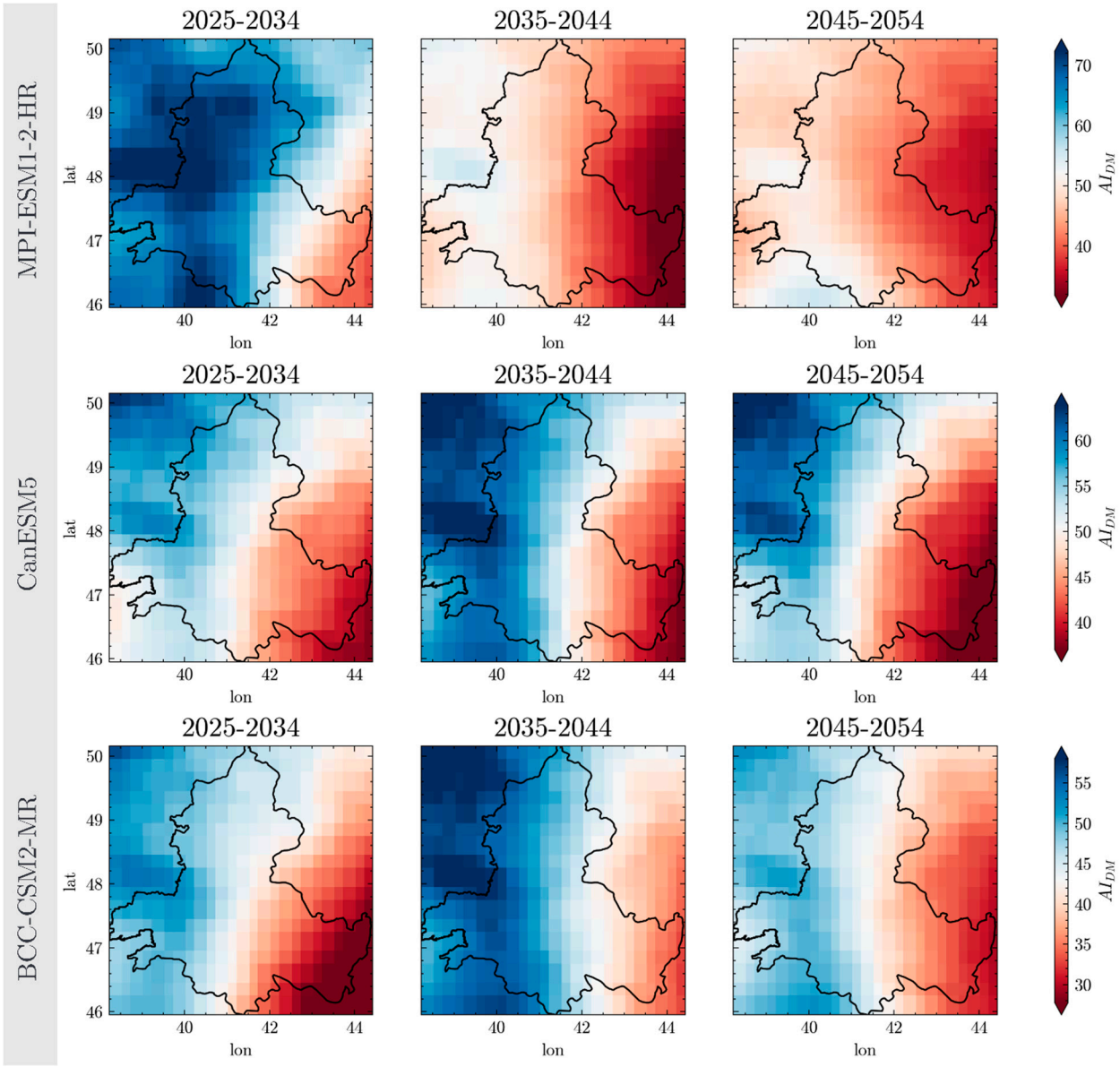


Figure 10. Spatial distribution of the De Martonne index according to global climate models MPI-ESM1-2-HR, CanESM5, and BCC-CSM2-MR in the Rostov region for ten-year periods from 2025 to 2054.

The CanESM5 and BCC-CSM2-MR models show similar results of De Martonne aridity index calculations, except that the CanESM5 model gives a forecast of wetter conditions than BCC-CSM2-MR. Regarding aridity, both models agree in predicting that it will gradually decline after a sharp increase in 2025–2034. However, the CanESM5 model predicts a sharper differentiation between dry and wet areas than the BCC-CSM2-MR.

According to the MPI-ESM1-2-HR model, by the year 2054, 65% of the Rostov region is expected to transition from the humid category (index > 60) to the sub-humid class. The most substantial changes are anticipated in the northern region, where the index is expected to decrease from 60 to 40 units. In contrast, the CanESM5 model demonstrates a stabilization scenario, in which 100% of the region's territory remains in the sub-humid class (30–60 units). The BCC-CSM2-MR model presents the most optimistic scenario, with minimal changes not exceeding ±5.6% in all regions. Notably, the models have not demonstrated the prediction of any region's transition to dry subhumid conditions (index < 30), which prevents the formation of critical level aridization. The southeastern

region remains the most vulnerable zone in all climate scenarios, with minimum index values ranging from 25 to 45 units. The spatial contrast between the most humid and arid regions remains at the level of 15–25 index units in all models, thereby confirming the stability of the meridional aridity gradient.

4. Discussion

The results of the study indicate a pronounced and steady increase in the mean annual air temperature from 1951 to 2024. This increase has been particularly strong over the last two decades, confirming current global and regional trends. In recent years, average annual temperatures in Rostov Oblast have exceeded 11 °C, 2 °C higher than in the 1950s. However, the dynamics of precipitation do not show the same clearly pronounced trend as temperature. It is characterized by high interannual variability, with periods of both intense moisture and precipitation deficits. Spatial analysis revealed a stable temperature gradient from north to south, as well as uneven precipitation distribution, with the greatest amounts falling in the southwest and the least in the southeast. The De Martonne aridity index also reflects spatial and temporal heterogeneity. After a period of active growth associated with high levels of precipitation in the last two decades, there has been a decrease, especially in the southeast. This indicates the strengthening of aridization processes in the southern part of the Rostov region. Global climate model forecasts for the period 2025–2054 uniformly predict a gradual increase in temperature and precipitation; however, the intensity of this growth varies by model. The most radical scenarios suggest an intensification of climatic contrasts and an expansion of zones with insufficient moisture, particularly in the southeastern part of the region.

The obtained results of temperature change in Rostov Oblast are in full agreement with the findings of Nazarenko [25], who recorded an increase in mean annual temperature by 1.2 °C for the period 1966–2020. Also, the revealed spatial pattern of aridization, characterized by significant changes in the eastern regions, confirms the conclusions of Gudko [27], who found a significant decrease in the hydrothermal Selyaninov coefficient in the same regions of Rostov Oblast. At the same time, it should be noted that the tendency to an increase in precipitation predicted by all used models somewhat contradicts the conclusions of Medyanik [26], who assumed a steady decrease in precipitation. The predictions of MPI-ESM1-2-HR and CanESM5 models about the formation of the climatic dipole "wet west–dry east" are consistent with the concept of Greve and Seneviratne [8] about the redistribution of atmospheric moisture under global warming.

The identified climate trends and projections have a direct impact on the region's agro-industrial complex, which is likely to lead to a transformation of agricultural approaches in the future. Projected temperature increases of 2–3 °C by 2054 and increased aridization of the southeast will make it unprofitable to grow moisture-loving crops such as corn and soybeans. As noted by Gudko [31], the most optimal solution in this situation is to increase the share of sorghum, chickpea, and flax cultivation, which are quite well adapted to moisture deficit and relatively high temperatures. The trend of temperature increase in the next 30 years increases the risk of potential substitution of spring wheat cultivation instead of winter wheat due to an increase in the number of warm winters and winter thaws. It should also be noted that even with the projected increase in precipitation (up to 1200 mm/year in the west), its uneven distribution and evapotranspiration due to rising air temperatures are likely to increase reliance on irrigation. This could potentially lead to significant competition between agriculture and industry, especially for water intake from the Tsimlyansk reservoir, which is already declining by an estimated 1.2 m/year, causing a cascading effect of ecosystem transformation in the surrounding areas.

4.1. Crop Adaptation Strategies

A review of the results reveals that the southeastern part of Rostov Oblast (Kuma–Manych Depression) is characterized by a high risk of aridization (Table 3). The region is characterized by a variation in the De Martonne index, with other areas exhibiting a low risk level ranging from 45 to 70. According to the De Martonne index classification, the northwestern part of the region demonstrated the most positive conditions in the future, where the climate will shift to humid. The central, north central, and southwest regions have also been observed to demonstrate stable conditions, without any significant shifts in climate regime. This region constituted approximately 80% of the territory and can be classified as the zone of low aridization risk. This aspect can preserve the traditional structure of the crops with minimal adaptation measures. The basis of crop rotation should be corn, soybeans, and winter wheat, which have been demonstrated to grow effectively with a De Martonne index above 40–45 units. The cultivation of additional drought-resistant crops, such as sorghum and chickpeas, is recommended as insurance crops, with a target area of 10–15% of grain production. This approach is expected to ensure diversification of risks without the need for a radical change in agro-industrial specialization.

Table 3. Proposed crop adaptation strategies in Rostov Oblast.

Zone	Risk Level	Main Crops	Supplementary Crops	Adaptation Level
West North Central Southwest	Low	corn, soybeans, winter wheat	Sorghum (drought resisted crops)	Minimal
Southeast	High	Sorghum, chickpeas	Winter wheat (limited)	Significant

The high-risk zone, which is in the southeastern part of the region, requires substantial adaptation measures. With an average index of 38 units, the primary crops should be sorghum and chickpeas, which have demonstrated effective adaptation to conditions with an index of 25–40 units. Intensive adaptation is required only in the southeastern regions (Zavetinsky, Zimovnikovsky, Orlovsky, Remontnensky), where it is necessary to convert 50–70% of grain areas to sorghum and leguminous crops within 3–5 years.

4.2. Limitations of the Study

The main limitation of this study is that the use of ERA5 reanalysis data is associated with systematic overestimation of precipitation amounts in 40% of cases, which is confirmed by comparison with correction data from weather stations [56]. Also, forecast calculations based on CMIP6 models have several limitations related to the lack of consideration of regional peculiarities of land use and anthropogenic impact, underestimation of uncertainty of inter-model discrepancies when extrapolating to 2054, and limited ability to reproduce extreme droughts [57]. The comparative analysis revealed some discrepancies in precipitation forecasts between models, which are particularly pronounced for the western parts of the region, most likely due to fundamental differences in the parameterization of convective processes in the model kernels. Also, this study does not take into account microclimatic effects of urbanized areas (Rostov-on-Don, Taganrog), where heat islands can enhance local aridization [58]. These limitations do not reduce the scientific value of the work but define directions for further research in the field of regional climate modeling.

The systematic overestimation of ERA5 precipitation [59,60] represents a structural limitation of the study, potentially leading to an overestimation of the De Martonne index and an underestimation of the degree of aridity. The spatial heterogeneity of this bias has the potential to distort the revealed aridity gradients, particularly in the arid southeastern

parts of the region. When interpreting the results, it is crucial to take this uncertainty into account, particularly when formulating adaptation strategies.

Despite this limitation, the utilization of ERA5 remains scientifically valid for the analysis of long-term trends, as systematic biases do not affect the slope of the time series, and qualitative conclusions about the direction of change remain valid [60]. Furthermore, the consistency of results across different CMIP6 models underscores the reliability of the identified aridification trends.

The utilization of NEX-GDDP-CMIP6 data offers high-quality regional projections. However, it is important to note that the methodology employed is subject to certain limitations. The BCSD method is predicated on the assumption that the relative spatial patterns observed from 1960 to 2014 will remain constant in the context of future climate changes. This stationary assumption can be violated by significant changes in atmospheric circulation. Furthermore, the bias correction does not affect the slope of the trends in the model projections, thereby preserving the original rates of change, as evidenced by the results obtained. The uncertainty of the downscaling data is estimated at ±10–15% for regional climate projections of continental areas.

5. Conclusions

The present study was conducted to comprehensively assess the spatiotemporal dynamics of climatic aridization in the Rostov region. This analysis was based on two sources of data: historical data from 1951 to 2024 and predictive climate models CMIP6 from 2025 to 2054. The primary results of the study are as follows.

The average annual air temperature in the Rostov region for the period 1951–2024 demonstrates a stable positive trend, especially pronounced since the early 2000s. By 2023, the values had increased to 12 °C, which is 2–3 °C higher than the values recorded in the 1950s. Precipitation demonstrates high interannual variability without a discernible long-term trend; however, a downward trend has been observed over the past two decades, particularly in the southeastern regions, leading to an increase in the continentality of the climate.

A stable meridional temperature gradient has been revealed. The southern parts of the region, adjacent to the Sea of Azov, have been found to be 1–2 °C warmer than the northern parts. The distribution of precipitation and the De Martonne aridity index both demonstrate the zonality of aridization, indicating that the driest conditions are observed in the southeast (Manych Lowland), while the northwestern regions remain relatively more humid.

All models utilized (MPI-ESM1-2-HR, CanESM5, BCC-CSM2-MR) indicate further warming by 2054 (+1.5–3 °C), but the intensity of changes varies. The CanESM5 model predicts the most significant temperature increase (up to 13–14 °C), while MPI-ESM1-2-HR and BCC-CSM2-MR demonstrate more temperate scenarios. Precipitation forecasts indicate a potential increase of 1000–1300 mm/year, characterized by significant spatial variability. Western regions are expected to experience increased precipitation, while southeastern regions are projected to undergo a moisture deficit.

According to the MPI-ESM1-2-HR model, by the year 2054, most of the Rostov region territory will transition from the humid category (index > 60) to the sub-humid class. The most substantial changes are anticipated in the northern region, where the index is expected to decline. The CanESM5 model presents a stabilization scenario, wherein 100% of the region's territory remains in the sub-humid class (30–60 units).

The findings indicate that 80% of the region's territory can be classified as a low climate risk zone, where the traditional cropping structure can be sustained with minimal adaptation measures. The foundation of crop rotation should be corn, soybeans, and

winter wheat. A recent analysis indicates that only 20% of the territory, specifically the southeastern zone, necessitates substantial adaptation measures in order to facilitate the transition to drought-resistant crops, such as sorghum and chickpeas. It is recommended that a gradual introduction of drought-resistant crops as insurance be implemented (10–15% of grain areas) for all zones in order to diversify risks.

Rising temperatures will increase evaporation and evapotranspiration, which, in conjunction with an uneven distribution of precipitation, will increase the dependence on irrigation. This necessitates a comprehensive review of water management strategies, particularly in light of the persistent decline in the Tsimlyansk reservoir, which is experiencing an annual reduction of 1.2 m. The projected increase in aridization in the southeastern regions will pose a significant challenge to the viability of cultivating moisture-loving crops, necessitating the development of adapted livestock farming practices, particularly in the areas of sheep and goat breeding.

Funding: This research received no external funding.

Data Availability Statement: The original contributions presented in this study are included in the article. Further inquiries can be directed to the corresponding author.

Conflicts of Interest: The authors declare no conflicts of interest.

References

1. Yao, J.; Liu, H.; Huang, J.; Gao, Z.; Wang, G.; Li, D.; Yu, H.; Chen, X. Accelerated Dryland Expansion Regulates Future Variability in Dryland Gross Primary Production. *Nat. Commun.* **2020**, *11*, 1665. [CrossRef] [PubMed]
2. Coleine, C.; Delgado-Baquerizo, M.; DiRuggiero, J.; Guirado, E.; Harfouche, A.L.; Perez-Fernandez, C.; Singh, B.K.; Selbmann, L.; Egidi, E. Dryland Microbiomes Reveal Community Adaptations to Desertification and Climate Change. *ISME J.* **2024**, *18*, wrae056. [CrossRef] [PubMed]
3. Schlaepfer, D.R.; Bradford, J.B.; Lauenroth, W.K.; Munson, S.M.; Tietjen, B.; Hall, S.A.; Wilson, S.D.; Duniway, M.C.; Jia, G.; Pyke, D.A.; et al. Climate Change Reduces Extent of Temperate Drylands and Intensifies Drought in Deep Soils. *Nat. Commun.* **2017**, *8*, 14196. [CrossRef] [PubMed]
4. Burrell, A.L.; Evans, J.P.; De Kauwe, M.G. Anthropogenic Climate Change Has Driven over 5 Million Km^2 of Drylands towards Desertification. *Nat. Commun.* **2020**, *11*, 3853. [CrossRef] [PubMed]
5. Lewin, A.; Murali, G.; Rachmilevitch, S.; Roll, U. Global Evaluation of Current and Future Threats to Drylands and Their Vertebrate Biodiversity. *Nat. Ecol. Evol.* **2024**, *8*, 1448–1458. [CrossRef] [PubMed]
6. Spinoni, J.; Barbosa, P.; De Jager, A.; McCormick, N.; Naumann, G.; Vogt, J.V.; Magni, D.; Masante, D.; Mazzeschi, M. A New Global Database of Meteorological Drought Events from 1951 to 2016. *J. Hydrol. Reg. Stud.* **2019**, *22*, 100593. [CrossRef] [PubMed]
7. Romanello, M.; Walawender, M.; Hsu, S.-C.; Moskeland, A.; Palmeiro-Silva, Y.; Scamman, D.; Ali, Z.; Ameli, N.; Angelova, D.; Ayeb-Karlsson, S.; et al. The 2024 Report of the Lancet Countdown on Health and Climate Change: Facing Record-Breaking Threats from Delayed Action. *Lancet* **2024**, *404*, 1847–1896. [CrossRef] [PubMed]
8. Greve, P.; Seneviratne, S.I. Assessment of Future Changes in Water Availability and Aridity. *Geophys. Res. Lett.* **2015**, *42*, 5493–5499. [CrossRef] [PubMed]
9. Muñoz-Sabater, J.; Dutra, E.; Agustí-Panareda, A.; Albergel, C.; Arduini, G.; Balsamo, G.; Boussetta, S.; Choulga, M.; Harrigan, S.; Hersbach, H.; et al. ERA5-Land: A State-of-the-Art Global Reanalysis Dataset for Land Applications. *Earth Syst. Sci. Data* **2021**, *13*, 4349–4383. [CrossRef]
10. Titkova, T.B.; Ananicheva, M.D. Using ERA5-Land Reanalysis and Data from Weather Stations in the Mountainous Regions of Russia to Assess Changes in the Glacial Systems of Eastern Siberia and the Far East. *Ice Snow* **2023**, *63*, 199–213. [CrossRef]
11. Seifu, T.K.; Eshetu, K.D. Characterizing the Aridity Indices and Potential Evapotranspiration Using CMIP6-GCMs in Two Distinct Regions of Ethiopia. *J. Water Clim. Change* **2024**, *15*, 1507–1531. [CrossRef]
12. Jafarpour, M.; Adib, A.; Lotfirad, M.; Kisi, Ö. Spatial Evaluation of Climate Change-Induced Drought Characteristics in Different Climates Based on De Martonne Aridity Index in Iran. *Appl. Water Sci.* **2023**, *13*, 133. [CrossRef]
13. Zhang, L.; Zhao, Y.; Cheng, T.F.; Lu, M. Future Changes in Global Atmospheric Rivers Projected by CMIP6 Models. *J. Geophys. Res. Atmos.* **2024**, *129*, e2023JD039359. [CrossRef]
14. Wu, F.; Jiao, D.; Yang, X.; Cui, Z.; Zhang, H.; Wang, Y. Evaluation of NEX-GDDP-CMIP6 in Simulation Performance and Drought Capture Utility over China—Based on DISO. *Hydrol. Res.* **2023**, *54*, 703–721. [CrossRef]

15. Li, X.; Tan, J.; Wang, X.; Shang, Q.; Li, H.; Li, X. Analysis of Future Drought Risk and Wheat Meteorological Disaster in Ningxia (Northwest China) Based on CMIP6 and SPEI. *Agronomy* **2024**, *14*, 3051. [CrossRef]
16. Taguela, T.N.; Pokam, W.M.; Dyer, E.; James, R.; Washington, R. Low-Level Circulation over Central Equatorial Africa as Simulated from CMIP5 to CMIP6 Models. *Clim. Dyn.* **2024**, *62*, 8333–8351. [CrossRef]
17. Fu, Y.; Lin, Z.; Guo, D. Improvement of the Simulation of the Summer East Asian Westerly Jet from CMIP5 to CMIP6. *Atmos. Ocean. Sci. Lett.* **2020**, *13*, 550–558. [CrossRef]
18. Zivanovic, S.; Gocic, M. The influence of climatic conditions on the occurrence of large forest fires: A case study of Stara Planina Nature Park in 2007 and 2019. *J. Appl. Life Sci. Environ.* **2023**, *56*, 195–209. [CrossRef]
19. Derdous, O.; Tachi, S.E.; Bouguerra, H. Spatial Distribution and Evaluation of Aridity Indices in Northern Algeria. *Arid Land Res. Manag.* **2021**, *35*, 1–14. [CrossRef]
20. Sales, E.S.G.; Matsunaga, W.K.; Braga, C.C.; Sakamoto, M.S.; Lucena, D.B.; de Brito, J.I.B. Climate classification for Northeast Brazil using reanalysis data and the Absolute Aridity Index. *Rev. Bras. Geogr. Física* **2024**, *17*, 1478–1500. [CrossRef]
21. Liu, C.; Yang, C.; Yang, Q.; Wang, J. Spatiotemporal Drought Analysis by the Standardized Precipitation Index (SPI) and Standardized Precipitation Evapotranspiration Index (SPEI) in Sichuan Province, China. *Sci. Rep.* **2021**, *11*, 1280. [CrossRef] [PubMed]
22. Vicente-Serrano, S.M.; Beguería, S.; López-Moreno, J.I. A Multiscalar Drought Index Sensitive to Global Warming: The Standardized Precipitation Evapotranspiration Index. *J. Clim.* **2010**, *23*, 1696–1718. [CrossRef]
23. Nkemelang, T.; New, M.; Zaroug, M. Temperature and Precipitation Extremes under Current, 1.5 °C and 2.0 °C Global Warming above Pre-Industrial Levels over Botswana, and Implications for Climate Change Vulnerability. *Environ. Res. Lett.* **2018**, *13*, 065016. [CrossRef]
24. Stefanidis, S.; Tegos, A.; Alexandridis, V. How Has Aridity Changed at a Fir (Abies Borisii-Regis) Forest Site in Central Greece during the Past Six Decades? *Environ. Sci. Proc.* **2023**, *26*, 121. [CrossRef]
25. Nazarenko, O. Regional Climate Change in the South of Rostov Region: A Case of Arid Steppe. *E3S Web Conf.* **2023**, *407*, 02006. [CrossRef]
26. Medyanik, N.; Cherednichenko, O.; Dovgotko, N.; Rybasova, Y. Climatic Adaptation as Priority of Sustainable Development of the Agrifood System in the Southern Regions of Russia. *BIO Web Conf.* **2021**, *37*, 00118. [CrossRef]
27. Gudko, V.N.; Usatov, A.V.; Azarin, K.V. Analysis of Hydrothermal Conditions in the Rostov Region in the Period 1960–2019. *Arid Ecosyst.* **2021**, *11*, 337–342. [CrossRef]
28. Nazarenko, O.V. Moisture Changes in the Rostov Region in 1966–2019. *UNNCRNSS* **2022**, *4*, 45–52. [CrossRef]
29. Bezuglova, O.S.; Golozubov, O.M.; Poluyan, D.I. Regional Features of Desertification Processes in Rostov Oblast. *Arid Ecosyst.* **2015**, *5*, 10–13. [CrossRef]
30. Novikova, A.F. Ameliorative Status of Irrigated Soils in Rostov Oblast. *Eurasian Soil Sci.* **2008**, *41*, 529–541. [CrossRef]
31. Gudko, V.; Usatov, A.; Ioshpa, A.; Denisenko, Y.; Shevtsova, V.; Azarin, K. Agro-Climatic Conditions of the Southern Federal District of Russia in the Context of Climate Change. *Theor. Appl. Clim.* **2021**, *145*, 989–1006. [CrossRef]
32. Oleg, B.; Nikolaevich, S.P. Effective Activity of Small Agricultural Regional Entrepreneurship as the Basis for Forming Food Independence of the Country. *Mosc. Econ. J.* **2024**, *9*, 180–191. [CrossRef]
33. Brock, G. COVID and Sanctions Resiliency in a Russian Region: The Case of Rostov Oblast 2010–2022. *J. East-West Bus.* **2024**, *30*, 114–132. [CrossRef]
34. Mandzhieva, S.S.; Goncharova, L.Y.; Batukaev, A.A.; Minkina, T.M.; Bauer, T.V.; Shertnev, A.K.; Chaplygin, V.A.; Sushkova, S.N.; Poluektov, E.V.; Burachevskaya, M.V.; et al. Current State of Haplic Chernozems in Specially Protected Natural Areas of the Steppe Zone. *OnLine J. Biol. Sci.* **2017**, *17*, 363–371. [CrossRef]
35. Pivovarov, S.; Popova, O. Russian Farmers Fight to Salvage Harvest as Major Region Cuts Forecast. *TimesLIVE*, 16 July 2024. Available online: https://www.timeslive.co.za/news/world/2024-07-17-russian-farmers-fight-to-salvage-harvest-as-major-region-cuts-forecast/ (accessed on 3 July 2025).
36. Agapkin, A.M.; Makhotina, I.A. The Grain Market of Russia. *IOP Conf. Ser Earth Environ. Sci.* **2021**, *839*, 022023. [CrossRef]
37. Novikov, A.; Pakhomova, A. Level of Fisheries Development and Its Impact on the Socio-Economic Development of the Region. *E3S Web Conf.* **2020**, *175*, 13017. [CrossRef]
38. Udalov, A.; Udalova, Z. The Analysis of Foreign Economic Activity of Agricultural Producers of the Southern Federal District. *E3S Web Conf.* **2020**, *193*, 01064. [CrossRef]
39. De Martonne, E. Pénéplaine ou Pénéplan. *Bull. L'association Géographes Français* **1925**, *2*, 1–2. [CrossRef]
40. Dikareva, T.V.; Rymyantsev, V.Y.; Soldatov, M.S.; Malkhazova, S.M. Medicinal Plants of Arid and Semiarid Biomes of Russia. *Arid Ecosyst.* **2021**, *11*, 62–72. [CrossRef]
41. Jamali, Z.; Heidarizadi, Z. Future Changes in Dry Conditions Using Statistical Downscaling Model (SDSM) in the Western Region of Gorgan Plain, Iran. *Arid Ecosyst.* **2022**, *12*, 345–352. [CrossRef]

42. Kazeev, K.S.; Kozun, Y.S.; Samokhvalova, L.S.; Kolesnikov, S.I. Influence of Aridity and Continentality of Climate on Soil Biological Properties in Transect of Rostov-on-Don–Astrakhan. *Izv. Akad. Nauk SSSR Ser. Geogr.* **2015**, *5*, 46–53. [CrossRef]
43. Gutjahr, O.; Putrasahan, D.; Lohmann, K.; Jungclaus, J.H.; von Storch, J.-S.; Brüggemann, N.; Haak, H.; Stössel, A. Max Planck Institute Earth System Model (MPI-ESM1.2) for the High-Resolution Model Intercomparison Project (HighResMIP). *Geosci. Model Dev.* **2019**, *12*, 3241–3281. [CrossRef]
44. Swart, N.C.; Cole, J.N.S.; Kharin, V.V.; Lazare, M.; Scinocca, J.F.; Gillett, N.P.; Anstey, J.; Arora, V.; Christian, J.R.; Hanna, S.; et al. The Canadian Earth System Model Version 5 (CanESM5.0.3). *Geosci. Model Dev.* **2019**, *12*, 4823–4873. [CrossRef]
45. Xin, X.; Zhang, J.; Zhang, F.; Wu, T.; Shi, X.; Li, J.; Chu, M.; Liu, Q.; Yan, J.; Ma, Q.; et al. *BCC BCC-CSM2MR Model Output Prepared for CMIP6 CMIP*; World Data Center for Climate: Hamburg, Germany, 2018.
46. Ferreiro-Lera, G.-B.; Penas, Á.; del Río, S. Unveiling Deviations from IPCC Temperature Projections through Bayesian Downscaling and Assessment of CMIP6 General Circulation Models in a Climate-Vulnerable Region. *Remote Sens.* **2024**, *16*, 1831. [CrossRef]
47. Ferreira, V.; Bonfim, O.T.; Mortarini, L.; Valdes, R.H.; Costa, F.D.; Maroneze, R. Atmospheric Blocking Events over the Southeast Pacific and Southwest Atlantic Oceans in the CMIP6 Present-Day Climate. *Climate* **2024**, *12*, 84. [CrossRef]
48. Adelodun, B.; Ahmad, M.J.; Odey, G.; Adeyi, Q.; Choi, K.S. Performance-Based Evaluation of CMIP5 and CMIP6 Global Climate Models and Their Multi-Model Ensembles to Simulate and Project Seasonal and Annual Climate Variables in the Chungcheong Region of South Korea. *Atmosphere* **2023**, *14*, 1569. [CrossRef]
49. Xie, W.; Wang, S.; Yan, X. Diurnal Temperature Range in Winter Wheat–Growing Regions of China: CMIP6 Model Evaluation and Comparison. *Theor. Appl. Clim.* **2023**, *152*, 123–134. [CrossRef]
50. Reboita, M.S.; Willian de Souza Ferreira, G.; Gabriel Martins Ribeiro, J.; Ali, S. Assessment of Precipitation and Near-Surface Temperature Simulation by CMIP6 Models in South America. *Environ. Res. Clim.* **2024**, *3*, 025011. [CrossRef]
51. Xiao, H.; Zhuo, Y.; Sun, H.; Pang, K.; An, Z. Evaluation and Projection of Climate Change in the Second Songhua River Basin Using CMIP6 Model Simulations. *Atmosphere* **2023**, *14*, 1429. [CrossRef]
52. Azad, N.; Ahmadi, A. Assessment of CMIP6 Models and Multi-Model Averaging for Temperature and Precipitation over Iran. *Sci. Rep.* **2024**, *14*, 24165. [CrossRef] [PubMed]
53. Virgin, J.G.; Fletcher, C.G.; Cole, J.N.S.; von Salzen, K.; Mitovski, T. Cloud Feedbacks from CanESM2 to CanESM5.0 and Their Influence on Climate Sensitivity. *Geosci. Model Dev.* **2021**, *14*, 5355–5372. [CrossRef]
54. Thrasher, B.; Maurer, E.P.; McKellar, C.; Duffy, P.B. Technical Note: Bias Correcting Climate Model Simulated Daily Temperature Extremes with Quantile Mapping. *Hydrol. Earth Syst. Sci.* **2012**, *16*, 3309–3314. [CrossRef]
55. Thrasher, B.; Wang, W.; Michaelis, A.; Melton, F.; Lee, T.; Nemani, R. NASA Global Daily Downscaled Projections, CMIP6. *Sci. Data* **2022**, *9*, 262. [CrossRef] [PubMed]
56. Grigorev, V.Y.; Frolova, N.L.; Kireeva, M.B.; Stepanenko, V.M. Spatial and Temporal Variability of ERA5 Precipitation Accuracy over Russia. *Izv. Ross. Akad. Nauk. Seriya Geogr.* **2022**, *86*, 435–446. [CrossRef]
57. Zhang, J.; Wu, T.; Li, L.; Furtado, K.; Xin, X.; Xie, C.; Zheng, M.; Zhao, H.; Zhou, Y. Constraint on Regional Land Surface Air Temperature Projections in CMIP6 Multi-Model Ensemble. *npj Clim. Atmos. Sci.* **2023**, *6*, 85. [CrossRef]
58. Sklyarenko, G.Y.; Shehurdin, G.R. Features of the Thermal Field of the City of Rostov-on-Don According to Remote Sensing Data. *UNNCRNSS* **2024**, 97–104. [CrossRef]
59. Zhou, Z.; Chen, S.; Li, Z.; Luo, Y. An Evaluation of CRA40 and ERA5 Precipitation Products over China. *Remote Sens.* **2023**, *15*, 5300. [CrossRef]
60. Lavers, D.A.; Hersbach, H.; Rodwell, M.J.; Simmons, A. An Improved Estimate of Daily Precipitation from the ERA5 Reanalysis. *Atmos. Sci. Lett.* **2024**, *25*, e1200. [CrossRef]

Disclaimer/Publisher's Note: The statements, opinions and data contained in all publications are solely those of the individual author(s) and contributor(s) and not of MDPI and/or the editor(s). MDPI and/or the editor(s) disclaim responsibility for any injury to people or property resulting from any ideas, methods, instructions or products referred to in the content.